PRAMANA — journal of physics | © Indian Academy of Sciences | Vol. 82, No. 1
January 2014
pp. 15–27

High-power Yb-doped continuous-wave and pulsed fibre lasers

B N UPADHYAYA
Solid State Laser Division, Raja Ramanna Centre for Advanced Technology, Indore 452 013, India
E-mail: bnand@rrcat.gov.in

DOI: 10.1007/s12043-013-0639-8; ***e*****Publication:** 5 January 2014

Abstract. High-power laser generation using Yb-doped double-clad fibres with conversion efficiencies in excess of 80% have attracted much attention during the last decade due to their inherent advantages in terms of very high efficiency, no misalignment due to in-built intracore fibre Bragg gratings, low thermal problems due to large surface to volume ratio, diffraction-limited beam quality, compactness, reliability and fibre-optic beam delivery. Yb-doped fibres can also provide a wide emission band from ∼1010 nm to ∼1170 nm, which makes it a versatile laser medium to realize continuous-wave (CW), Q-switched short pulse, and mode-locked ultrashort pulse generation for various applications. In this article, a review of Yb-doped CW and pulsed fibre lasers along with our study on self-pulsing dynamics in CW fibre lasers to find its role in high-power fibre laser development and the physical mechanisms involved in its generation has been described. A study on the generation of high-power CW fibre laser of 165 W output power and generation of high peak power nanosecond pulses from acousto-optic Q-switched fibre laser has also been presented.

Keywords. Continuous-wave fibre laser; Q-switched fibre laser; nonlinearity; thermal effects; self-pulsing; Yb-doped fibre; nanosecond pulse

PACS Nos 42.55.Wd; 42.60.Pk; 42.60.Gd; 42.65.−k

1. Introduction

High-power CW fibre lasers are required mainly for material processing and defence applications. Cladding pumped fibre lasers, which use double-clad fibre architecture and can produce single-mode laser output without requiring single-mode diode pump sources are most widely used for generating kW-level CW output powers. In view of this, there has been a growing interest in high-power Yb-doped fibre lasers as a potential replacement for bulk solid-state lasers in many applications. In addition, fibre lasers also have inherent advantages in terms of higher efficiency, single-mode output, long life of maintenance-free operation, no cooling requirement, and no risk of misalignment by means of intracore fibre Bragg grating mirrors. Further, the wide absorption band of

Yb-doped fibres from ∼800 to ∼1064 nm and lasing wavelengths from ∼974 to ∼980 nm and ∼1010 to ∼1160 nm makes it a unique laser source for various applications. There are several reports on the generation of kW level of CW output power from Yb-doped fibre lasers [1,2]. There is a recent report from IPG Photonics about the development of up to 10 kW single-mode CW output from an ytterbium fibre laser at 1075 nm with record brightness, which can be considered as the most intense CW laser of any kind (http://www.ipgphotonics.com). With such intense lasers, it is possible to undertake most of the material processing applications. Thus, for high-power CW laser generation, it is necessary to optimize the pumping geometry and the resonator configuration based on an analysis of pump and signal evolution. High-power output from the fibre laser is normally generated using oscillator only or master oscillator power amplifiers (MOPA) or by means of coherent or incoherent beam combination from several fibre lasers. However, in scaling output power to kilowatt level, issues such as heat load management of doped fibre, photo-darkening, self-pulsing along with heat load on splice joints become extremely important.

Further, Q-switched and mode-locked fibre lasers can be used in micromachining, range finding, remote sensing, laser marking, laser surgery and to pump optical parametric oscillators which require short and high peak power pulses. Realization of actively Q-switched multi-moded fibre laser output providing pulse energy as high as 7.7 mJ at 500 Hz repetition frequency and 250 ns pulse duration using a 60 μm large core diameter double-clad Yb-doped fibre with $M^2 = 7$ has already been reported by Renaud *et al* [3]. Single-moded output with a pulse energy of 1.2 mJ at 10 kHz repetition rate and 37 ns pulse duration using a 40 μm core diameter fibre has also been reported by Piper *et al* [4]. Due to the high peak power of the Q-switched pulse that is confined in a fibre core of small cross-sectional area and a long fibre cavity, many non-linear effects such as self-phase modulation (SPM), cross-phase modulation (XPM), stimulated Raman scattering (SRS), and stimulated Brillouin scattering (SBS) play a crucial role in their performance [5]. In such Q-switched fibre lasers, SRS can result in the generation of narrower Raman pulses, and transfer of the pulse energy from the lasing signal wave to Raman–Stokes waves. SBS can provide strong feedback to the laser cavity in the form of a short and unstable Brillouin-scattered relaxation pulse. SPM can lead to spectral broadening of the optical pulses and XPM may affect the evolutions of the signal, Brillouin and Raman pulses in the Q-switching process. The small core area of the fibre with a tight mode confinement leads to a high gain for a relatively small amount of energy stored in the gain medium (in the form of excited Yb ions). The high gain leads to losses via amplified spontaneous emission or even spurious lasing between pulses. This limits the pulse energy that can be stored in the gain medium and thus the energy of the output pulse from a Q-switched fibre laser [6].

In this article, a review of basic issues related to the generation of high power from Yb-doped CW and pulsed fibre lasers will be presented. It will also provide results of our study on self-pulsing dynamics in Yb-doped CW fibre laser along with generation of high-power laser output from CW and Q-switched fibre lasers. Due to the wide scope of ultrashort mode-locked pulsed fibre lasers, this article has been confined to the review of Q-switched pulses only. Section 2 covers the basics related to the Yb-doped fibre lasers and § 3 covers the study on CW fibre laser and its self-pulsing dynamics. Sections 4 and 5 cover high-power Yb-doped CW fibre laser and acousto-optic Q-switched Yb-doped fibre lasers, respectively.

2. Basics related to Yb-doped fibre lasers

To understand high-power laser generation from Yb-doped fibre lasers, we shall go through some of the basics related to Yb-doped fibre lasers, which are listed below:

2.1 *Energy level structure and pump absorption*

Figure 1 shows the energy level diagram of Yb ion in silica fibre. Yb possesses a simple atomic structure with only two principal manifolds, i.e., ground level ($^2F_{7/2}$) and an excited state ($^2F_{5/2}$) separated by $\sim$10000 cm^{-1}, which makes it an ideal rare-earth element for lasing. The three sublevels of the upper $^2F_{5/2}$ manifold are labeled as 'e', 'f', and 'g' and the four sublevels of the lower $^2F_{7/2}$ manifold are labelled as 'a', 'b', 'c', and 'd'. Weak multi-phonon decay is practically the only non-radiative channel that exists. The excited state has a lifetime of $\sim$1 ms and acts as metastable level. The absence of higher energy levels near the upper manifold reduces the occurrence of multi-photon relaxation and excited state absorption (ESA). Yb ions are pumped into the sublevels of the $^2F_{5/2}$ manifold and laser emission results by transition from sublevel 'e' of $^2F_{5/2}$ manifold to sublevels 'a', 'b', 'c', and 'd' of $^2F_{7/2}$ manifold. Figure 1 shows the absorption and emission cross-sections of Yb-doped aluminosilicate glass for a doping concentration of 1.134×10^{20} atoms/cm^3. Pumping can, in principle, be done in a broad range from 900 nm to 1060 nm, while gain can be realized at the 975 nm peak or around the secondary peak starting from $\sim$1020 nm to $\sim$1150 nm. However, there are two main absorption peaks: one at 915 nm for excited state transition a$\rightarrow$f and the other at 975 nm for transition a$\rightarrow$e. For pumping at 915 nm, lasing transition can occur from level e$\rightarrow$a at $\sim$975 nm or from level e$\rightarrow$b, 'c', or 'd' in the range 1020–1150 nm. For pumping at 975 nm, lasing transition can occur from level e$\rightarrow$b, 'c', or 'd' in the range 1020–1150 nm. For lasing transition below $\sim$990 nm, it acts as a true three-level system and for lasing from $\sim$1020 nm to $\sim$1150 nm, it acts as a quasifour-level system.

For high-power fibre lasers, low threshold is not of concern. In contrast to fibre communication systems, where fibres are required to have small single-mode cores, small cores turn out to be an obstacle in the generation of high power laser outputs. Pumping of single-clad single-mode fibre requires single-mode laser-diode pump sources, and the output from single-mode pigtailed diodes is normally limited to below 1 W. Hence, the output from single-clad single-mode fibre lasers is also limited to below 1 W. The clad

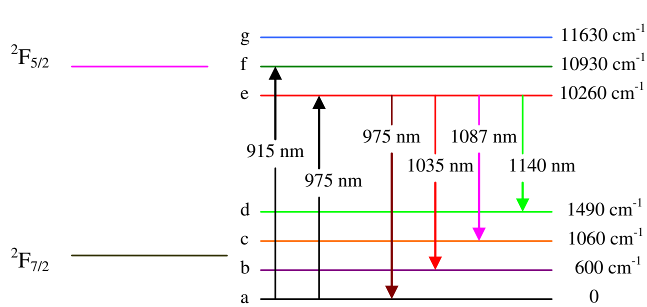

Figure 1. Energy level diagram of Yb ion in silica.

pumping technology using double-clad fibre structure was developed as a solution for this limitation. A typical double-clad fibre is designed in such a way that the core supports a large-area fundamental mode for efficient absorption of the pump; the inner cladding is of a larger diameter and high numerical aperture for efficient coupling from multimode diode bars. The shape of the inner cladding is normally non-circular to achieve better absorption of the pump in the doped core region. Figure 2 shows different inner clad shapes of rare-earth-doped fibres. Thus, cladding-pumped fibre lasers can be treated as devices to generate diffraction-limited single-mode laser output using multimode pump lasers. With large size inner cladding, very high pump powers can be launched into a double-clad fibre. However, the core size limits the output power to a certain level due to the onset of optical damage and thermal effects. Figure 3 shows the schematic of a double-clad fibre laser configuration. In this figure, blue angled arrows show the unabsorbed pump radiation emitting in a cone corresponding to NA of the inner cladding. At the input end, the red arrow shows pump axis and the blue arrows show schematically the acceptance of pump light in a cone angle corresponding to NA of the inner cladding.

2.2 *Thermal effects*

Quantum defect is the main source for heat deposition in active fibres. Although active fibres used in fibre lasers have large surface to active volume ratio, thermal management becomes a critical issue in scaling high output power from Yb-doped double clad fibres. Since polymer coating is used to guide inner clad pump light and also acts as protective layer for Yb-doped double clad fibres, onset of thermal damage or degradation of outer coating is a limiting factor in high-power fibre lasers. Outer coating used in double clad fibres is normally made of fluorinated polymer, which can withstand a maximum temperature of about 200°C, and 80°C is the safe limit for long term reliability. The maximum heat deposition density in the core, $P_{h\,\max}$, without the onset of coating damage is given by [7]

$$P_{h\,\max} \approx 4\pi (T_{\rm d} - T_{\rm s}) \left[\frac{2}{K_{\rm oc}} \log_{\rm e}\left(\frac{r_{\rm oc}}{r_{\rm ic}}\right) + \frac{2}{r_{\rm oc} h} \right]^{-1}, \tag{1}$$

where $T_{\rm d}$ is the maximum temperature that the coating can tolerate, $T_{\rm s}$ is the temperature of the surroundings, $K_{\rm oc}$ is the thermal conductivity of the outer cladding, $r_{\rm oc}$ is the radius of the outer cladding, $r_{\rm ic}$ is the radius of the inner cladding, and h is the heat transfer

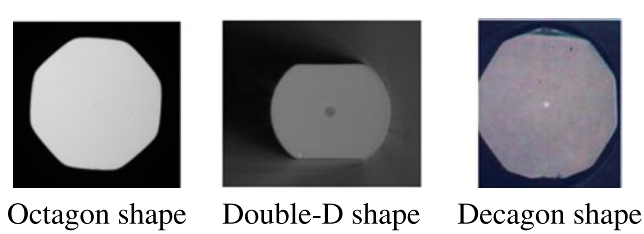

Figure 2. Cross-sectional images of a few inner cladding shapes used in double-clad fibre lasers.

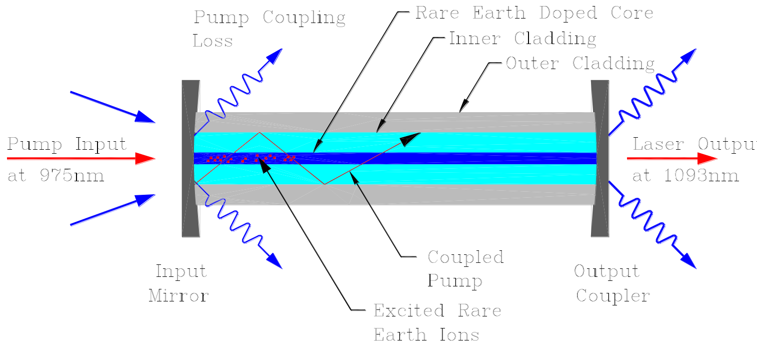

Figure 3. Schematic of a double-clad fibre laser configuration.

coefficient. From eq. (1), it is clear that maximum heat deposition depends on heat transfer coefficient and hence on heat sinking configuration and it is favourable to use large diameter fibres for power scaling. Thus, it is extremely important to manage heat load in high-power fibre lasers.

2.3 *Nonlinearity*

Nonlinear effects play a key role in generating high power from fibre lasers. SRS is a major limiting factor in kW-level CW and Q-switched pulsed fibre lasers, whereas SBS is a major limiting factor in single-frequency fibre lasers. Further, SPM has a major role in ultrashort pulsed fibre laser systems. Thresholds for the onset of SRS and SBS are given by [5]

$$(P_{0\mathrm{cr}})_{\mathrm{SRS}} \approx \frac{16A_{\mathrm{eff}}}{g_{\mathrm{R}}L_{\mathrm{eff}}}, \tag{2}$$

$$(P_{0\mathrm{cr}})_{\mathrm{SBS}} \approx \frac{21A_{\mathrm{eff}}}{g_{\mathrm{B}}L_{\mathrm{eff}}}\left[1+\frac{\Delta\upsilon_{\mathrm{s}}}{\Delta\upsilon_{\mathrm{B}}}\right], \tag{3}$$

where A_{eff} is the effective core area and L_{eff} is the effective fibre length given by

$$L_{\mathrm{eff}} = \frac{1}{\alpha_{\mathrm{s}}}\left[1-\exp\left(-\alpha_{\mathrm{s}}L\right)\right]. \tag{4}$$

The Brillouin and Raman gain coefficients in silica are $g_{\mathrm{B}} = 5\times10^{-11}$ m/W and $g_{\mathrm{R}} = 1\times10^{-13}$ m/W, respectively [5]. $\Delta\upsilon_{\mathrm{B}} \approx 30$ MHz is the Brillouin gain bandwidth and $\alpha_{\mathrm{s}} \approx 5\times10^{-3}$ m^{-1} is the scattering loss at the signal wavelength. Thus, it is important to manage these nonlinear effects while generating high-power CW and pulsed fibre lasers.

3. CW fibre laser and self-pulsing dynamics

High-power CW Yb-doped fibre lasers with stable output power are of interest for various applications, such as pump source for other lasers and optical parametric oscillators, in spectroscopy and in the study of nonlinear phenomenon. However, it is not easy to achieve a truly CW fibre laser having stable output power (without fluctuations). Under CW pumping conditions, it is normally expected to have a CW output from fibre lasers. However, in several CW pumped rare-earth doped fibre lasers, for different resonator configurations and pumping geometries, self-pulsation in the output has been reported [8,9]. Two types of self-pulsations in fibre lasers are reported in the literature: sustained self-pulsing (SSP) and self-mode locking (SML). SSP refers to the emission of high-intensity pulses at irregular intervals, whereas SML refers to the laser output modulation or 'spiking' in the output with period corresponding to the cavity round-trip time. Several possible mechanisms such as ion-pairing acting as a saturable absorber, re-absorption of laser photons in the unpumped part of the doped fibre, external perturbation such as pump noise, relaxation oscillations of the inversion and photon populations, interaction between laser signal and population inversion, distributed Rayleigh scattering, cascaded stimulated Brillouin scattering (SBS), and other nonlinear effects (stimulated Raman scattering (SRS), self-phase modulation (SPM), cross-phase modulation (XPM), and four-wave mixing (FWM)) as the sources of self-modulation and self-pulsing in different rare-earth-doped fibre lasers have been reported [10–12]. Techniques to exploit self-pulsing to achieve regular narrow pulses with enhanced Q-switching have also been reported. There have also been substantial efforts to eliminate self-pulsing. The reported techniques to suppress self-pulsing include the use of unidirectional fibre ring cavity, use of a low transmission output coupler to realize a high Q-cavity, resonant pumping near the lasing wavelength to prevent rapid depletion of gain, thereby minimizing relaxation oscillations, electronic feedback to the pump laser to shift the gain and phase, increasing the cavity round-trip time by adding a long section of passive fibre to change the dynamics of relaxation oscillation, using fast saturable gain of a semiconductor optical amplifier within the fibre laser cavity, and use of the narrow pass-band of a $\lambda/4$-shifted FBG structure in a ring cavity to limit the number of longitudinal cavity modes [13,14]. Although efforts were considerable to understand and control self-pulsing phenomenon in fibre lasers, there is plenty of scope for research and in-depth understanding of the physical parameters responsible for this phenomenon.

For studying CW laser generation and self-pulsing dynamics, three different Fabry–Perot resonator configurations, shown in figures 4a–4c, were used [15–17]. The experimental set-up consisted of a Yb-doped double-clad fibre having a core diameter of 10 μm with a numerical aperture (NA) of 0.075, and an inner clad diameter of 400 μm with an NA of 0.46. This Yb-doped fibre had an octagonal inner clad geometry and clad-pump absorption of 0.8 dB/m at 975 nm. A 20 W fibre-coupled laser diode with centre wavelength 975 nm was used to pump 18 m length of the Yb-doped fibre. The pump laser output from the 200 μm core fibre pigtail was collimated using a lens of 25 mm focal length and then focussed using another lens of 25 mm focal length to image the pump fibre end on to the input end of the doped fibre. The doped fibre was cleaved at the ends to sustain higher damage thresholds.

Figure 4a shows the high-finesse forward pumping configuration in which the dichroic mirror is kept between the two lenses used for coupling pump light into the doped fibre; the cleaved end with $\sim$4% Fresnel reflection at the farther fibre end of the doped fibre acts as the output coupler. Figure 4b shows the high-finesse backward pumping configuration in which two dichroic mirrors have been

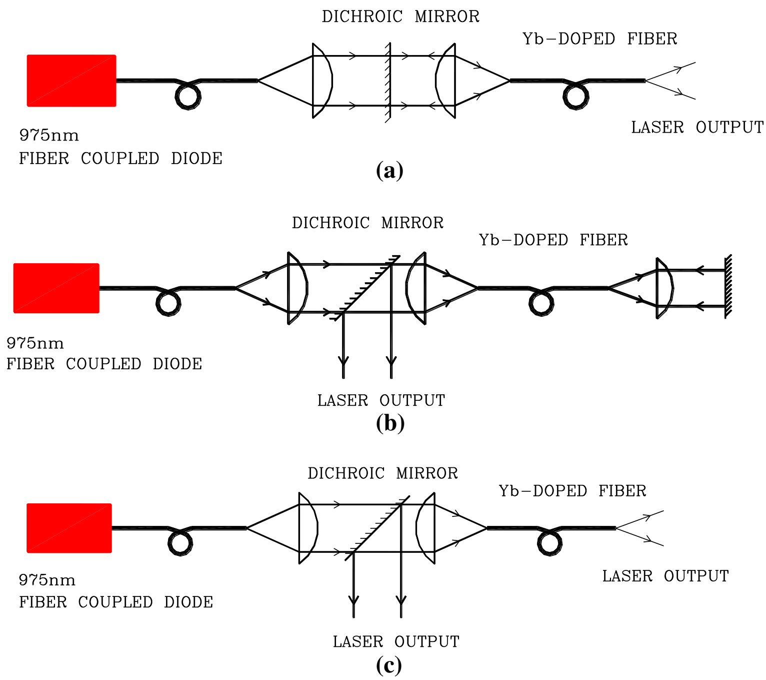

Figure 4. (**a**) High-finesse forward pumping configuration in which output power is taken from the farther end. (**b**) High-finesse backward pumping configuration in which output power is taken from the pumping end using the tilted dichroic mirror. (**c**) Low-finesse resonator configuration.

used; the cleaved end with ∼4% Fresnel reflection from the pump input end of the doped fibre acts as the output coupler. Figure 4c shows the low-finesse fibre laser resonator configuration, and in this case the cleaved ends with ∼4% Fresnel reflection from both the fibre ends act as the Fabry–Perot cavity mirrors. The dichroic mirror used in these configurations is highly transmitting at 975 nm and highly reflecting (∼98%) in the wavelength range 1064–1140 nm. A maximum output power of 10.75 W was achieved at an input pump power of 17.2 W, with a slope efficiency of ∼73% and an optical-to-optical conversion efficiency of 62.5%, in the backward pumping configuration. The laser output was in single transverse mode with diffraction-limited beam quality, and was emitted in a full cone angle of 150 mrad, defined by the NA of the doped fibre.

In the case of low-finesse resonator configuration, experimentally it was observed that the CW output power from both the ends ceases to increase beyond 1.8 W, and starts fluctuating due to the occurrence of strong random self-pulsing. With further increase in the pump power, the peak power of these random pulses increased, and an increase in the fluctuation about the average output power was observed. Figure 5a shows the observed random self-pulsing and figure 5b shows the expanded view of one of the random pulses with pulse duration less than 25 ns, for an input pump power of 8 W. As

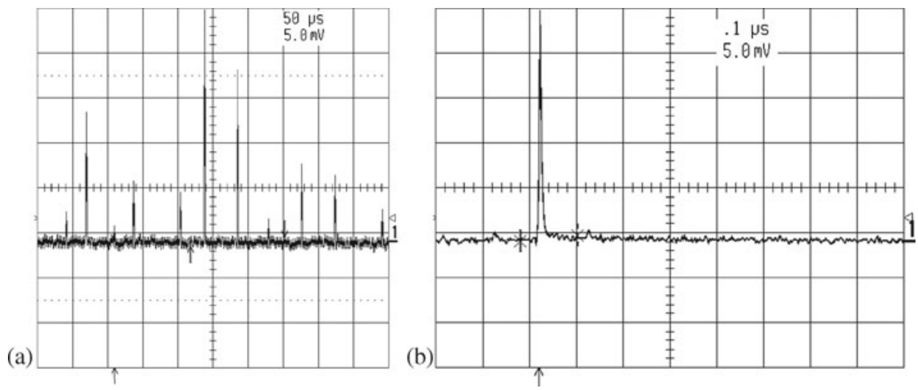

Figure 5. (**a**) Output of the fibre laser, showing random self-pulses in the case of the low-finesse cavity, for an input pump power of 8 W. (**b**) An expanded oscilloscope trace of one of the random self-pulses.

the pulses are random in time, and their peak powers are not constant, the (measured) average power keeps fluctuating. Self-pulsing was also observed for high-finesse forward- and backward-pumping configurations, but the peak power of these self-pulses was very low compared to that for low-finesse cavity, and a decrease in the peak power of these self-pulses occurred with increase in pump power. This is due to the increase in gain uniformity along the fibre length with increase in pump power. Figure 6 shows the output spectrum before and after the onset of random self-pulsing. It shows the presence of nonlinear SRS and SBS effects with the presence of first- and second-order Stokes lines shifted from the main laser line.

As the degree of non-uniformity of steady-state gain profile is different for high- and low-finesse cavities, these cavities will respond differently to the distributed backscattered noise in the form of RS and SBS or any other pump-induced noise. Further, weak random self-pulsing in high-finesse resonator with forward- and backward-pumping configurations, and strong random self-pulsing in low-finesse cavity shows that highly non-uniform steady-state gain profile with the gain peaking at some point along fibre length, and consequent build-up of random pulse from RS and SBS noise in the case of low-finesse cavity, is essentially responsible for strong random self-pulsing. Thus, to avoid or reduce self-pulsing, it is important to use high-finesse cavity.

Experimental results also show that self-pulsing is initiated as soon as the lasing starts. By increasing the pump power, population inversion in the weakly pumped portion increases and density of atoms in the doped fibre for signal re-absorption decreases, which results in an increase in initial transmission through the weakly pumped portion and reduction in saturable absorption. The reduction in the peak power of self-pulses at higher pump input is also observed experimentally. As the saturable absorption is distributed along the fibre length, period of self-pulsing is random in contrast to regular passively Q-switched output [15,16].

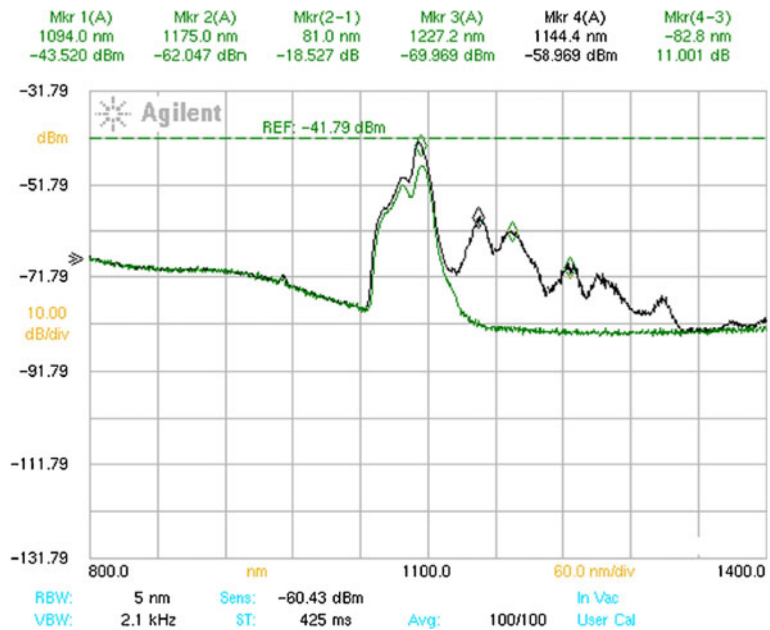

Figure 6. Output spectrum in case of low-finesse cavity; the lower trace shows spectrum before the onset of random self-pulsing ($Pp(0) = 2.5$ W) and the upper trace shows the spectrum after the onset of strong random self-pulsing ($Pp(0) = 8$ W).

4. High-power Yb-doped CW fibre laser

The experimental set-up consists of a large mode area (LMA) Yb-doped double-clad active fibre with a core diameter of 20 μm and an inner clad diameter of 400 μm. Pump absorption for inner clad launching of the pump beam at 975 nm is 1.7 dB/m. Both the ends of the Yb-doped fibre were perpendicularly cleaved and the fibre was coiled on a metallic mandrel to remove heat load from the active fibre. Fourteen fibre pigtailed diodes of 30 W output power at 975 nm with pigtail fibre core diameter of 200 μm and 0.22 NA were selected to pump from both the ends of the Yb-doped fibre using 7:1 multimode pump combiners. Temperature of all the diodes was maintained at 25°C for the whole range of its operations using water-cooled heat sinks for its mounting. Fibre pigtails of seven such diodes were fusion spliced individually with seven pump input ports of multimode pump combiner using Vytran GPX-3400 fusion splicing workstation. Maximum transmission of ∼86% was achieved with optimized splice joints. Two such diode pump modules were made (see figure 7) and used to pump from both ends of the Yb-doped double-clad fibre using two fibre-optic pump combiners. Pump beam from the output port of each pump combiner was collimated using a plano-convex lens and then it was imaged at the Yb-doped fibre using another plano-convex lens. Both the ends of the Yb-doped fibre were held in temperature-controlled metallic V-grooves to prevent possible thermal damage to the gain fibre coating by any over-filled pump or signal power, or by the heat generated in the gain fibre due to non-radiative emission

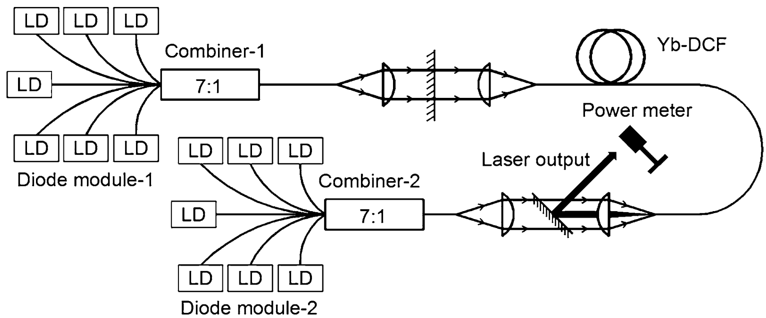

Figure 7. A schematic of 165 W Yb-doped CW fibre laser.

processes. A dichroic mirror with high transmission (HT) at 975 nm and high reflectivity (HR) of ∼100% in broadband from 1040 to1100 nm for normal incidence has been placed at one end of the Yb-doped double-clad fibre between the two lenses for signal feedback. This mirror along with the other cleaved end of the Yb-doped fibre providing 4% Fresnel reflection act as resonator mirrors. Another dichroic mirror with HT at 975 nm and HR in a broadband from 1040 to 1100 nm at 25° angle of incidence has been placed between the two lenses to take out the laser beam from resonator. Figure 8 shows a schematic of the experimental set-up. Using this set-up an output power of 165 W was achieved at the combined maximum input pump power of 316 W from both the ends with an optical-to-optical conversion efficiency of 52% and a slope efficiency of 56.5%. Figure 8 shows the output spectrum at the maximum output power of 165 W. The output spectrum is peaked at 1079.7 nm with spread from 1064.1 nm to 1100.1 nm and FWHM line width of ∼7 nm. Another peak near 975 nm in the output spectrum shows pump wavelength.

In this scheme, we have used a few bulk optics components in Yb-doped fibre laser oscillator. However, we are trying to use fibre Bragg grating mirrors to make it all-fibre nature. Further scaling of the output power has been planned by using amplifier stages with MOPA configuration to achieve kilowatt level of output power in future.

5. Acousto-optic Q-switched fibre laser

When a laser beam of frequency ω is allowed to pass through an acousto-optic cell at Bragg angle (which is almost perpendicular to the direction of propagation of the acoustic wave of frequency Ω), diffraction of the beam takes place. The laser beam is diffracted to a single order if the beam is incident at an angle equal to the Bragg angle (θ_B) given by

$$\sin\theta_B = \frac{\lambda_0}{2n_0\Lambda},$$

where n_0 is the refractive index of the medium, λ_0 is the free space optical wavelength, and Λ is the acoustic wavelength. Diffracted beam in the +1 order will have a frequency $\omega + \Omega$ and the diffraction efficiency will depend on acoustic intensity, interaction length, and figure of merit of the acousto-optic material. When the AO Q-switch is placed inside the laser resonator and RF power is switched on, a fraction of the energy of the laser

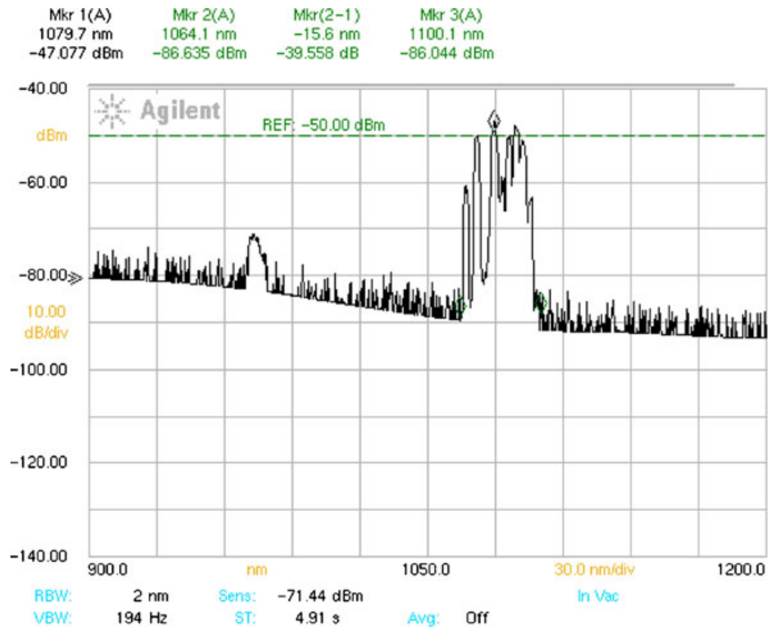

Figure 8. Yb-doped CW fibre laser output spectrum at the maximum output power of 165 W.

radiation is diffracted out of the resonator, resulting in cavity loss that prevents laser action. When the RF power is switched off, full transmission through the Q-switch cell is restored and a laser pulse is emitted. If the RF power is modulated at a certain repetition rate, laser pulses also get generated at the same repetition rate, and the process is termed as Q-switching.

Figure 9 shows the experimental set-up used in the study of AO Q-switched fibre laser. A 20 W fibre-coupled laser diode emitting at 975 nm was used to pump 18 m of the Yb-doped double-clad fibre with a core diameter of 10 μm and a numerical aperture (NA) of 0.075; the octagonal inner cladding has a diameter of 400 μm with a NA of 0.46, enabling an efficient end-pumping configuration. The laser resonator consisted of a Fabry–Perot cavity with a rear mirror of ∼100% reflectivity and 4% Fresnel reflection at the other cleaved end, which forms the output coupler. A dichroic mirror, which is

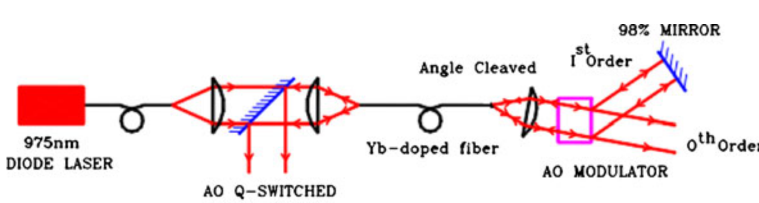

Figure 9. Experimental set-up to study Q-switched fibre laser. The dashed line at the fibre end indicates the plane of cleaving of the fibre end at an angle.

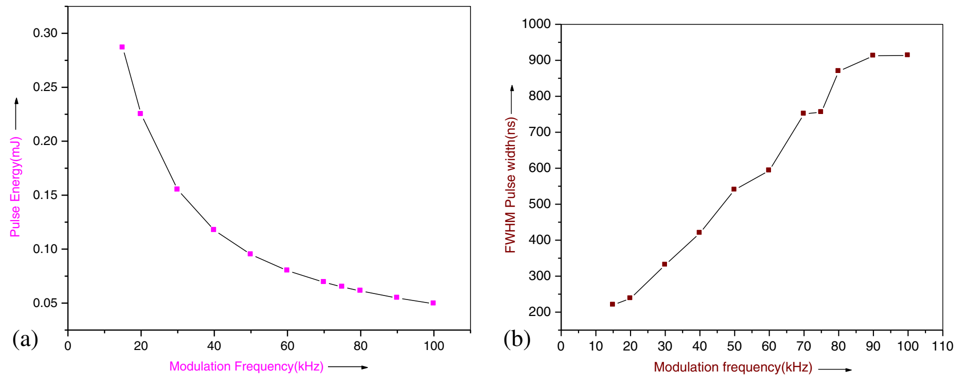

Figure 10. (**a**) Measured pulse energy and (**b**) measured FWHM pulse width as a function of modulation frequency.

highly transmitting at 975 nm and highly reflecting in the wavelength band from 1064 nm to 1140 nm, was used to take out the Q-switched laser beam. To achieve faithful Q-switching operation, one of the fibre ends has been angle-polished at 10° to prevent any feedback that could result in spurious lasing between the pulses. The AO switch operated at a radio frequency of 27.12 MHz with 1–100 kHz modulation rate, and a variable duty cycle was applied in the study of Q-switching action. The AO modulator, which was kept near the rear mirror end, provided a diffraction efficiency of about 60% with a deflection angle of 7.68 mrad. With RF modulation, the first-order beam was either fully present or absent and therefore a faithful Q-switching was achieved with first-order diffracted beam. At the maximum pump power of 17.2 W, stable pulses were achieved in the modulation range 15–100 kHz. At lower repetition rates, i.e. in the range 1–15 kHz, it was required to sufficiently lower the pump power to achieve stable pulses. Figures 10a and 10b show the measured pulse energy and pulse width as a function of modulation frequency. A maximum pulse energy of 285 μJ was achieved with a pulse duration of 220 ns at 15 kHz modulation frequency. Figure 11a shows oscilloscope trace typical AO Q-switched pulse and figure 11b shows repetitive occurrence of AO Q-switched pulses at 20 kHz of modulation frequency [18,19].

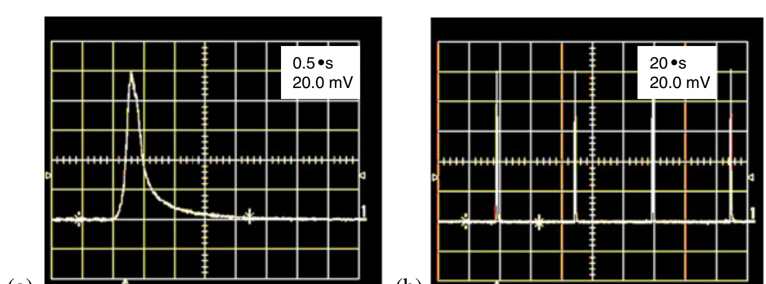

Figure 11. Oscilloscope trace of (**a**) typical AO Q-switched pulse and (**b**) repetitive occurrence of AO Q-switched pulses at 20 kHz of modulation frequency.

6. Conclusion

In conclusion, issues related to the generation of high-power CW and pulsed fibre lasers have been given in this article. A study of self-pulsing dynamics in Yb-doped CW fibre lasers to find its role in high-power fibre laser development and the physical mechanisms involved in its generation have been presented. This study resulted in finding ways of suppression for self-pulsing in high-power fibre lasers, and consequent development of 165 W of Yb-doped CW fibre laser oscillator. Results of our study on acousto-optic Q-switched fibre lasers have also been presented.

References

[1] Y Jeong, J K Sahu, D N Payne and J Nilsson, *Opt. Express* **12**, 6088 (2004)

[2] Y Fan, Bing He, Jun Zhou, Jituo Zheng, Houkang Liu, Yunrong Wei, Jingxing Dong and Qihong Lou, *Opt. Express* **19**, 15162 (2011)

[3] C C Renaud *et al*, *7.7 mJ pulses from a large core Yb-doped cladding pumped Q-switched fiber laser*, CLEO 2001, p. 219, 6–11 May 2001

[4] A Piper *et al*, *1.2 mJ, 37 ns single-moded pulses at 10 kHz repetition rate from a Q-switched ytterbium fibre laser*, CLEO 2003, Vol. 1, p. 2, 16–21 May 2004

[5] G P Agrawal, *Nonlinear fibre optics*, 2nd edn (Academic Press, San Diego, 1995)

[6] C C Renaud *et al*, *IEEE J. Quantum Electron.* **37**, 199 (2001)

[7] J W Kim, D Y Shen, J K Sahu and W A Clarkson, *IEEE J. Sel. Top. Quantum Electron.* **15**, 361 (2009)

[8] A Hideur, T Chartier, C Ozkul and Francois Sanchez, *Opt. Commun.* **186**, 311 (2000)

[9] F Brunet, Y Taillon, P Galarneau and S LaRochelle, *J. Lightwave Technol.* **23**, 2131 (2005)

[10] B Ortac *et al*, *Opt. Commun.* **215**, 389 (2003)

[11] A Hideur *et al*, *Opt. Commun.* **186**, 311 (2000)

[12] P Glas, *Opt. Commun.* **161**, 345 (1999)

[13] H Chen, G Zhu, Niloy K Dutta and Kevin Dreyer, *Appl. Opt.* **41**, 3511 (2002)

[14] A Suzuki, Y Takahashi, M Yoshida and M Nakazawa, *IEEE Photonics Technol. Lett.* **19**, 1463 (2007)

[15] B N Upadhyaya, Usha Chakravarty, A Kuruvilla, M R Shenoy, K Thyagarajan and A K Nath, *Opt. Commun.* **281**, 146 (2008)

[16] B N Upadhyaya, Usha Chakravarty, A Kuruvilla, S M Oak, M R Shenoy and K Thyagarajan, *Opt. Commun.* **283**, 2206 (2010)

[17] B N Upadhyaya, A Kuruvilla, Usha Chakravarty, M R Shenoy, K Thyagarajan and S M Oak, *Appl. Opt.* **49**, 2316 (2010)

[18] B N Upadhyaya, Usha Chakravarty, A Kuruvilla, K Thyagarajan, M R Shenoy and S M Oak, *Opt. Express* **15**, 11576 (2007)

[19] B N Upadhyaya, Arun Kumar, Usha Chakravarty, S M Oak, M R Shenoy and K Thyagarajan, *IEEE J. Quantum Electron.* **47(6)**, 786 (2011)